Hindawi
Mathematical Problems in Engineering
Volume 2022, Article ID 5485130, 14 pages
https://doi.org/10.1155/2022/5485130

Research Article

A 2D Model Which Accounts for Transverse Strains in a Linear Elastic Thick Shell

Nzengwa Robert,[1,2] Djopkop Kouanang Landry,[1,2] Bodol Momha Merlin,[2] Amba Jean Chills,[1,2] Nkongho Anyi Joseph,[2,3] and Zoa Ambassa[1,2]

[1]*Ecole Nationale Supérieure Polytechnique de Douala BP 2701, Douala, Cameroon*
[2]*Laboratory of Energy Materials Modeling and Methods (E3M), Douala, Cameroon*
[3]*Higher Technical Teacher Training College of Kumba, PO Box 249 Buea Road, Kumba, Cameroon*

Correspondence should be addressed to Djopkop Kouanang Landry; landriville35@gmail.com

Received 31 May 2022; Revised 5 September 2022; Accepted 6 October 2022; Published 18 October 2022

Academic Editor: Salvatore Caddemi

In this paper we present a 2D four-parameter model that accounts for the variation of transverse deformation through-the-thickness in thick linear elastic shells. This model is deduced directly from the 3D elasticity equations of the traction-displacement boundary value problem. Transverse shear strains and thickness variation are accountable through additional terms which appear in the final equations besides well-known terms in the classical Kirchhoff-Love models for thin shells. A unique solution of the variational equation is established, and numerical and analytical results are compared with satisfaction.

1. Introduction

Shell structures are increasingly being used in modern complex constructions. An outstanding problem is how to account for the through-the-thickness stretching and shear strains in a two-dimensional model when the shell becomes thick. Let $x = (x^1, x^2)$ be the coordinates of the generic point of the mid-surface of the shell, and z the transverse coordinate. In order to derive a 2D shell model from the 3D solid, a displacement of the form as shown in following equation was proposed in [1].

$$x = \varphi + \sum_{n=1}^{\infty} z^n d^n, \tag{1}$$

where d^n are the shell directors and φ the position vector of the mid-surface in the deformed configuration. Several attempts to approach the kinematics of a point on the shell are presented in the literature to offer 2D models, although there are also 3D models. These latter have the advantage of avoiding complex shell finite elements [2]. But numerically, a locking phenomenon arises when the thickness of the shell is small, and in addition, numerical approximation requires a voluminous mesh in three dimensions to approach the exact solution. The numerical implementation is memory-greedy and needs an extensive calculating time, hence the necessity to search for efficient 2D models. In this sense, several authors ([3–6]) have proposed 2D models based on the works of Love, Sander and Kirchhoff, where the proposed kinematics satisfy the Kirchhoff-Love hypotheses, i.e., normal segments to the mid-surface before deformation remain rigid and normal to the deformed mid-surface ($\varepsilon_{xz} = \varepsilon_{yz} = \varepsilon_{zz} = 0$). So, transverse strains do not contribute to the strain energy. Also, transverse shear stresses $\sigma^{\alpha 3}$ and the pinch stress σ^{33} are neglected. In [7], the nonlocal model of strain gradient small-scale approach and the first-order shear deformation shell theory (FSDST), initially proposed by Hencky, Timoshenko-Mindlin, Naghdi-Berry, and Reissner-Mindlin ([8–10]), which are 2D models were proposed. These models calculate transverse shear stresses but do not address variations in thickness (see ([11–13]). Some authors restricted the series of equation (1) into a linear or quadratic formula in z ([14–16]). In this case, the number of parameters (or unknown functions) of the model

is 6 or 7 unlike in thin shell theory where they are only 3. Moreover, the strain tensor which is a change in metrics, is either linear or quadratic in z and does not depend on the change of the fundamental forms of the mid-surface as expressed in ([17, 18]) for linear elastic thick shells. The N-T theory implemented in ([19–22]) proposed by [17] introduced the Gauss deformation strain tensor (change of the third fundamental form) and calculated the transverse stresses $\sigma^{xz}, \sigma^{yz}, \sigma^{zz}$ as reactions to a more general plane strain. The setting is quite different from that of the classical shell theory. However, it does not calculate transverse strains. In this paper we present a 2D model also derived from the 3D elasticity by introducing a particular form of admissible displacements obtained as a solution of a torsion loading problem in 3D solid. Let ϕ be the vector field representing the total transverse strains. We assume $\mathrm{rot}(\phi) = 0$ as widely used in 3D solids for torsion problems. The solution of the resulting ordinary differential equation is in-plane quadratic and depends transversally on a stretching function $q(x,z) = w(z)\overline{q}(x)$, $w(z)$ is a transverse distribution function. The displacement appears to be the sum of the plane strain thick shell displacement field [18] with a warping in-plane tensor and a through-the-thickness stretching term. The number of parameters is 4. The resulting 2D model accounts for transverse strains and stresses and appears to be an improvement on the linear elastic thick shell theory. Moreover, the transverse stretching can be described by a nonpolynomial function in z or a polynomial function of any order according to the desired accuracy. In the work of [23], a good conformity is observed between the experimental and numerical predictions for the choice of a linear polynomial distribution stretching function.

The rest of the paper is organized as follows: Section 2 is devoted to the study of the admissible displacement and its consequences on strains and constitutive laws. In Section 3 we establish the existence and uniqueness of the solution to a model problem, the classical traction-displacement variational problem which is the 2D model. We next present convergence tests and compare numerical and analytical results in Section 4. We conclude in Section 5 after some discussions.

The repeated index convention is adopted unless otherwise specified. The derivative of a function $\partial u/\partial x_i$ will also be denoted $u_{,i}$ or $\partial_i u$. Greek and Latin indexes range in $\{1,2\}$ and $\{1,2,3\}$ respectively. Covariant derivation will be denoted "|" or ∇ in the 3D shell and mid-surface respectively. The scalar product of matrices A and B will be denoted $A{:}\,B$. Further notations will be specified in the text.

2. Admissible Displacements and Constitutive Law

Let $\Omega = S \times [-h,h]$ (S is the mid-surface and $h>0$ is half the thickness) denote a shell. We assume the surface S is bounded and sufficiently smooth [24] for all subsequent computations. Let $\{a_1, a_2, a_3\}$ and $\{a^1, a^2, a^3\}$ denote the covariant and contravariant bases of the mid-surface and $\{G_1, G_2, G_3\}$, $\{G^1, G^2, G^3\}$ the covariant and contravariant bases of the shell. Then

$$\begin{aligned} x &= \left(x^1, x^2\right)G_\alpha = \left(\delta_\alpha^\gamma - z b_\alpha^\gamma\right)a_\gamma = (\mu)_\alpha^\gamma a_\gamma, \\ G_3 &= a_3 G^\alpha = \left(\delta_\gamma^\alpha - z b_\gamma^\alpha\right)^{-1} a^\gamma = \left(\mu^{-1}\right)_\gamma^\alpha a^\gamma, G^3 = a^3, \\ d\Omega &= (G_1, G_2, a_3)\mathrm{d}x^1\mathrm{d}x^2\mathrm{d}z = \left(1 - 2z\overline{H} + z^2\overline{K}\right)\mathrm{d}z\mathrm{d}S \\ &= \psi(x,z)\mathrm{d}z\mathrm{d}S; 2\overline{H} = b_\alpha^\alpha, \overline{K} = \det b, \end{aligned} \tag{2}$$

where $b_\alpha^\rho = a^{\rho\gamma}b_{\gamma\alpha}$ and $b_{\gamma\alpha}$ denote the curvature tensor components and $a^{\alpha\beta}$ is the contra variant component of the metric of the mid-surface S. We have implicitly assumed that the characteristic parameter of the mid-surface $\chi = h/R$ is less than 1; h is half the thickness and R the minimum absolute value of its radius of curvature. A vector field v: $\overline{\Omega} \longrightarrow \mathbb{R}^3$ can be expressed component wise indifferently in the G-base or the a-base as follows:

$$v = v_i(x,z)G^i = \overline{v}_\alpha(x,z)a^\alpha + v_3(x,z)a^3 \text{ and deduce that } v_\alpha = \mu_\alpha^\gamma \overline{v}_\gamma, \overline{v}_\alpha = \left(\mu^{-1}\right)_\alpha^\gamma v_\gamma. \tag{3}$$

Then the strain tensor [17] reads

$$\begin{aligned} \epsilon_{\alpha\beta}(v) &= \frac{\left(v_{\alpha|\beta} + v_{\beta|\alpha}\right)}{2} = \frac{\left[\mu_\alpha^\nu\left(\nabla_\beta \overline{v}_\nu - b_{\alpha\beta}\overline{v}_3\right) + \mu_\beta^\nu\left(\nabla_\alpha \overline{v}_\nu - b_{\nu\beta}\overline{v}_3\right)\right]}{2}, \\ \epsilon_{\alpha 3}(v) &= \frac{\left(v_{\alpha|3} + v_{3|\alpha}\right)}{2} = \frac{\left[\mu_\alpha^\nu \overline{v}_{\nu,3} + \left(\overline{v}_{3,\alpha} + b_\alpha^\nu \overline{v}_\nu\right)\right]}{2}, \epsilon_{33}(v) = v_{3,3} = \frac{\mathrm{d}v_3}{\mathrm{d}z}. \end{aligned} \tag{4}$$

We deduce the form of admissible displacement and strain from the following

Lemma 1. *Let $\phi(x^1, x^2, z) = (\phi_i)$ be such that $\phi_\alpha(x,z) = \epsilon_{\alpha 3} + \epsilon_{3\alpha} = 2\epsilon_{\alpha 3}, \phi_3(x,z) = \epsilon_{33}$. We suppose $rot(\phi) = 0$; $rot(\phi)_i = \phi_{i+1,i+2} - \phi_{i+2,i+1}$ mod [3]*

Then there exist functions $\xi_i(x)$ and $q(x,z)$ such that

$$
\begin{aligned}
v_\alpha &= \xi_\alpha - z\left(\partial_\alpha \xi_3 + 2b_\alpha^\rho \xi_\rho\right) + z^2\left(\left(b_\alpha^\rho b_\rho^\tau \xi_\tau + b_\alpha^\rho \partial_\rho \xi_3\right)\right), v_3 = \xi_3 + q(x,z),\\
\epsilon_{\alpha\beta}(v) &= e_{\alpha\beta}(\xi) - zk_{\alpha\beta}(\xi) + z^2 Q_{\alpha\beta}(\xi) + q(x,z)\Upsilon_{\alpha\beta}(x,z),\\
\epsilon_{\alpha 3}(v) &= \frac{\partial_\alpha q}{2}, \quad \epsilon_{33}(v) = \partial_z q,\\
e_{\alpha\beta}(\xi) &= \frac{\left(\nabla_\alpha \xi_\beta + \nabla_\beta \xi_\alpha - 2b_{\alpha\beta}\xi_3\right)}{2},\\
k_{\alpha\beta}(\xi) &= \nabla_\alpha b_\beta^\upsilon \xi_\upsilon + b_\alpha^\upsilon \nabla_\beta \xi_\upsilon + b_\beta^\upsilon \nabla_\alpha \xi_\upsilon + \nabla_\alpha \nabla_\beta \xi_3 - b_\alpha^\tau b_{\tau\beta}\xi_3,\\
Q_{\alpha\beta}(\xi) &= \frac{\left(b_\alpha^\upsilon \nabla_\beta\left(b_\upsilon^\tau \xi_\tau + \nabla_\upsilon \xi_3\right) + b_\beta^\upsilon \nabla_\alpha\left(b_\upsilon^\tau \xi_\tau + \nabla_\upsilon \xi_3\right)\right)}{2},\\
\Upsilon_{\alpha\beta}(x,z) &= -\frac{\left(\mu_\alpha^\nu b_{\nu\beta} + \mu_\beta^\nu b_{\nu\alpha}\right)}{2},
\end{aligned}
\tag{5}
$$

where e, k, and Q respectively change in the first, second, and third fundamental forms of the mid-surface and Υ is the section warping tensor, b_β^α the mixed components of the curvature tensor, $b_{\rho\alpha}$ the covariant components of the curvature tensor, and δ_α^ρ Kronecker's symbol.

Proof. We shall denote $(v_{3,1}, v_{3,2})$ by ∇v_3. Let

$$A_\beta^\alpha = \left(\mu^{-1}\right)_\beta^\alpha, \left(A^{-1}\right)_\beta^\alpha = \mu_\beta^\alpha. \tag{6}$$

The tensors A and b commute and we deduce from $AA^{-1} = I$ that $\mathrm{d}A/\mathrm{d}z = A^2 b$. From equation (2) we deduce that there exists $q(x,z)$ such that $\phi_i = \partial_i q$ which is equivalent to $\epsilon_{\alpha 3} = \partial_\alpha q/2, \epsilon_{33} = \partial_z q$ or

$$A^{-1}\frac{\mathrm{d}\overline{v}}{\mathrm{d}z} + b\overline{v} + \nabla v_3 = \nabla q, \frac{\mathrm{d}v_3}{\mathrm{d}z} = \partial_z q. \tag{7}$$

Equation (7) are also equivalent to

$$\frac{d(A\overline{v})}{\mathrm{d}z} + A^2\nabla(v_3 - q) = 0, \quad \frac{\mathrm{d}v_3}{\mathrm{d}z} = \partial_z q. \tag{8}$$

Let $w = \nabla(v_3 - q)$ then equation (8) becomes

$$\frac{d(A\overline{v})}{\mathrm{d}z} + A^2 w = 0, \frac{\mathrm{d}v_3}{\mathrm{d}z} = \partial_z q. \tag{9}$$

A solution to equation (9) is
$v_3 = \eta_3 + q, \overline{v} = A^{-1}\overline{\eta} - z\nabla\eta_3, \overline{\eta} = (\eta_1, \eta_2)$. In fact since $\mathrm{d}w/\mathrm{d}z = 0$, one has

$$
\begin{aligned}
d\frac{\left(A\left(A^{-1}\overline{\eta} - zw\right)\right)}{\mathrm{d}z} + A^2 w &= \frac{d(\overline{\eta} - zAw)}{\mathrm{d}z} + A^2 w = -zA^2 bw - Aw + A^2 w\\
&= -A^2\left(zb + A^{-1}\right)w + A^2 w\\
&= -A^2 w + A^2 w = 0.
\end{aligned}
\tag{10}
$$

Therefore,

$$\overline{v} = A^{-1}\overline{\eta} - z\nabla\eta_3, v_3 = \eta_3 + q, \tag{11}$$

or

$$
\begin{aligned}
v_\alpha &= \eta_\alpha - z\left(\partial_\alpha \eta_3 + 2b_\alpha^\rho \eta_\rho\right) + z^2\left(b_\alpha^\rho b_\rho^\tau \eta_\tau + b_\alpha^\rho \partial_\rho \eta_3\right), v_3\\
&= \eta_3 + q(x,z).
\end{aligned}
\tag{12}
$$

The solution v can be decomposed as a sum of two displacements namely a plane strain displacement field $v(\eta) = (v_\alpha(\eta), \eta_3)$ [17] and a stretching displacement $v(q) = (0,0,q)$. Therefore the strain can also be decomposed as

$$
\begin{aligned}
\epsilon_{ij}(v) &= \epsilon_{ij}(v(\eta)) + \epsilon_{ij}(v(q))\\
&= \epsilon^\eta + \epsilon^q,
\end{aligned}
\tag{13}
$$

where

$$\begin{aligned}
&\epsilon_{\alpha\beta}(v(\eta)) = e_{\alpha\beta}(\eta) - zk_{\alpha\beta}(\eta) + z^2 Q_{\alpha\beta}(\eta) = \epsilon^{\eta}_{\alpha\beta}, \epsilon_{i3}(v(\eta)) = 0 = \epsilon^{\eta}_{i3},\\
&\epsilon_{\alpha\beta}(v(q)) = q(x,z)\Upsilon_{\alpha\beta}(x,z) = \epsilon^{q}_{\alpha\beta},\\
&\epsilon_{\alpha 3}(v(q)) = \frac{\partial_\alpha q}{2} = \epsilon^{q}_{\alpha 3}, \epsilon_{33}(v(q)) = \partial_z q = \epsilon^{q}_{33},
\end{aligned} \tag{14}$$

and the proof is complete by taking $\eta = \xi$.

It should be noted that if $\phi = 0$, equation (2) will be satisfied. Therefore, plane strains hypothesis which leads to the N-T displacement is another form of equation (2). The in-plane displacement is quadratic in z with an additional warping strain. The stretching function can be expressed as follows:

$$q(x,z) = w(z)\overline{q}(x), \tag{15}$$

where w is an arbitrary nonconstant function or a polynomial of any degree. The number of unknown functions is 4.

Let us consider the strain decomposition $\epsilon = \epsilon^{\eta} + \epsilon^{q} = \epsilon(\eta) + \epsilon(q)$. For a linear elastic isotropic homogeneous material with Lamé constants $\overline{\lambda}, \overline{\mu}$, the stress-strain constitutive relations is as follows:

$$\begin{aligned}
\sigma &= \overline{\lambda}\left(\epsilon^{l}_{l}\right)G + 2\overline{\mu}\,\epsilon,\\
&= \sigma\left(\epsilon^{\eta}\right) + \sigma\left(\epsilon^{q}\right).
\end{aligned} \tag{16}$$

Since $\epsilon^{3}_{3}(\eta) = 0$, we have

$$\sigma^{33} = \overline{\lambda}\left(\epsilon^{\alpha}_{\alpha}(\eta) + \epsilon^{\rho}_{\rho}(q)\right) + (\overline{\lambda} + 2\overline{\mu})\epsilon^{3}_{3}(q). \tag{17}$$

If $\sigma^{33} = 0$, then

$$\begin{aligned}
\epsilon^{3}_{3} &= -\frac{\overline{\lambda}}{(\overline{\lambda} + 2\overline{\mu})}\left(\epsilon^{\alpha}_{\alpha}(\eta) + \epsilon^{\alpha}_{\alpha}(q)\right),\\
\sigma^{\alpha 3} &= 2\overline{\mu}\epsilon^{\alpha 3}(q),
\end{aligned} \tag{18}$$

and plane stress can be reproduced only if $\partial_\alpha q = 0$.

3. Presentation of the 2D Model

Let the border of S be partitioned by $\partial S = \gamma_0 \cup \gamma$ such that the border of the shell reads $\partial\Omega, = \Gamma_0 \cup, \Gamma_1 \cup, \Gamma_- \cup \Gamma_+; \Gamma_0 = \gamma_0 \times]-h, h; \Gamma_1 = \gamma_1 \times]-h, h; \Gamma_- = S \times \{-h\}; \Gamma_+ = S \times \{h\}$. The model problem is the standard traction-displacement boundary value problem defined by: find the displacement field u: $(x,z) \in \overline{\Omega} \longrightarrow \mathbb{R}^3$, ($\overline{\Omega}$ is the closure of Ω) which solves the following equations:

$$\begin{aligned}
&-\mathrm{div}\,\sigma = f \text{ in } \Omega,\\
&u(.) = 0 \text{ on } \Gamma_0, \sigma\overrightarrow{n} = p \text{ on } \Gamma = \Gamma_1 \cup \Gamma_- \cup \Gamma_+,\\
&\sigma^{ij} = \overline{\lambda}\epsilon^{l}_{l}(u)G^{ij} + 2\overline{\mu}\epsilon^{ij}(u),
\end{aligned} \tag{19}$$

where $\overrightarrow{n}$ is the unit outer normal vector; f^{ε}, p volume and surface force densities, respectively; $\mathrm{div}\sigma = (\sigma^{ij}_{j})$. The variational equation associated to the model problem reads: find $u \in \mathrm{IH}^{1}_{\Gamma_0}(\Omega) = \left\{v \in (H^1(\Omega))^3, v = 0 \text{ on } \Gamma_0\right\}$ such that

$$\begin{aligned}
&E(u,v) = L(v), \quad \text{for all } v \in IH^{1}_{\Gamma_0}(\Omega),\\
&E(u,v) = \int_\Omega \sigma^{ij}(u)\epsilon_{ij}(v)\mathrm{d}\Omega,\\
&L(v), = \int_\Omega f^i v_i \mathrm{d}\Omega + \int_\Gamma p^i v_i \mathrm{d}\Gamma,
\end{aligned} \tag{20}$$

$H^m(D)$ for a natural number $m \neq 0$ and a domain D in $\mathbb{R}^1, \mathbb{R}^2$ or $\mathbb{R}^3$ designates a Sobolev space; $H^0(D) = L^2(D)$. Volume and surface forces are supposed to be sufficiently regular.

The model problem has a unique solution because the operator $E(.,.)$ is coercive in the space of admissible displacements $IH^{1}_{\Gamma_0}(\Omega)$. We shall be interested in the particular case where $q(x,z) = w(z)\overline{q}(x)$. Let $U_{\mathrm{ad}} = \left\{v \in \mathrm{IH}^{1}_{\Gamma_0}(\Omega), \quad \mathrm{Rot}\,\phi = 0\right\}$, then U_{ad} is a closed subset of $\mathrm{IH}^{1}_{\Gamma_0}(\Omega)$. Let v be in U_{ad}, then because w is nonconstant in z, we deduce from (7) and the boundary condition on the displacement that $\eta_1 = \eta_2 = \eta_3 = \overline{q} = \partial_\alpha \eta_3 = 0 \text{ on } \gamma_0$. It is easy to check that

$$\begin{aligned}
&\eta_\alpha \in H^{1}_{\gamma_0}(S),\\
&\overline{q} \in H^{1}_{\gamma_0}(S),\\
&\eta_3 \in H^{2}_{\gamma_0}(S),\\
&H^{2}_{\gamma_0}(S) = \left\{\eta_3 \in H^2(S), \eta_3 = \partial_{\overrightarrow{\nu}}\eta_3 = 0 \text{ on } \gamma_0\right\},
\end{aligned} \tag{21}$$

$\overrightarrow{\nu}$ is the outer unit vector on the border of the mid-surface. We denote the set of admissible displacements and the bilinear form, respectively, by

$$\begin{aligned}
&U^{w}_{\mathrm{ad}} = \left\{(\eta,\overline{q}), \eta_\alpha \in H^{1}_{\gamma_0}(S), \overline{q} \in H^{1}_{\gamma_0}(S), \eta_3 \in H^{2}_{\gamma_0}(S)\right\},\\
&E(u,v) = E^{w}((\xi,\overline{q}), (\eta,\overline{\gamma})),
\end{aligned} \tag{22}$$

where $u = u(\xi, \overline{q})$, $v = v(\eta, \overline{y})$ are constructed as in equation (12).

Lemma 2. *The operator E^w is coercive in U^w_{ad}.*

Proof. Let $X = X(\eta, \overline{q}) \in U^w_{\text{ad}}$ then $e_{\alpha\beta}(\eta), k_{\alpha\beta}(\eta), Q_{\alpha\beta}(\eta), \overline{q}, \partial_1\overline{q}, \partial_2\overline{q} \in L^2(S)$. We next define

$$\begin{aligned} \|\overline{q}\|^2_{L^2(S)} &= \max\left\{\int_\Omega w^2(z)\overline{q}^2(x)\mathrm{d}\Omega, \int_\Omega w'^2(z)\overline{q}^2(x)\mathrm{d}\Omega\right\}, \\ \left\|\partial_\alpha\overline{q}\right\|^2_{L^2(S)} &= \int_\Omega w^2(z)\partial_\alpha\overline{q}^2(x)\mathrm{d}\Omega, \\ \overline{X} &= (e, k, Q, \overline{q}, \partial_1\overline{q}, \partial_2\overline{q}), \\ \Theta &= \left\{\overline{X} \in L^2(S)^3 \times L^2(S)^3 \times L^2(S)^3 \times L^2(S) \times L^2(S) \times L^2(S)\right\}, \end{aligned} \tag{23}$$

equipped with the norm

$$\|\overline{X}\| = \left(\|e\|^2 + \|k\|^2 + \|Q\|^2 + \|\overline{q}\|^2 + \left\|\partial_1\overline{q}\right\|^2 + \left\|\partial_2\overline{q}\right\|^2\right)^{1/2}, \tag{24}$$

where we have voluntarily omitted the subscript $L^2(S)$ on the norms. We deduce from the expression of the strain tensor that the bilinear form E^w can also be considered as a quadratic form on the space Θ where it is also continuous for the weak topology. Therefore, it is bounded in the unit ball and there exist positive constants m, M such that $m \le E^w(\overline{X}, \overline{X}) \le M$. We deduce that for all $X \in \Theta$, one has $m\|\overline{X}\|^2 \le E^w(\overline{X}, \overline{X}) \le M\|\overline{X}\|$. More over there exists $\overline{X}_m$ in the unit ball such that $E^w(\overline{X}_m, \overline{X}_m) = m$. We infer that $m>0$. In fact suppose $m = 0$. Then

$$\begin{aligned} 0 = E^w(\overline{X}_m, \overline{X}_m) &\ge 2\mu \\ &\left\{\int_\Omega \left(e_m - zk_m + z^2Q_m + w(z)\overline{q}_m\Upsilon\right): \left(e_m - zk_m + z^2Q_m + w(z)\overline{q}_m\Upsilon\right) + \left\|\overline{q}_m\right\|^2 + \left\|\partial_1\overline{q}_m\right\|^2 + \left\|\partial_2\overline{q}_m\right\|^2\right\}. \end{aligned} \tag{25}$$

We deduce that $\overline{q}_m = 0$ and from [17] we have $e_m = k_m = Q_m = 0$ which is in contradiction with $\|\overline{X}_m\| = 1$. Therefore $E^w(X, X) = E^w(\overline{X}, \overline{X}) \ge m\|\overline{X}\|^2$. Again from [17, 25] we deduce that there exists a strictly positive constant C such that $E^w(X, X) \ge C\|X\|^2$ and the proof is complete.

Theorem 1. *The 2D variational equation for the genuine traction-displacement problem has a unique solution $(\xi(x)\overline{q}(x))$ which satisfies the equations: find $(\xi(x), \overline{q}(x))$ such that $(\xi(.), \overline{q}(.)) \in U^w_{ad}$;*

$$\begin{aligned} E^w(u, v) &= L^w(v), v \in U^w_{\text{ad}}, \\ u_\alpha &= \xi_\alpha(x) - z\left(\partial_\alpha\xi_3(x) + 2b^\rho_\alpha\xi_\rho(x)\right) + z^2\left(b^\rho_\alpha b^\tau_\rho\xi_\tau(x) + b^\rho_\alpha\partial_\rho\xi_3(x)\right), \\ u_3 &= \xi_3(x) + w(z)\overline{q}(x), \\ v_\alpha &= \eta_\alpha - z\left(\partial_\alpha\eta_3 + 2b^\rho_\alpha\eta_\rho\right) + z^2\left(b^\rho_\alpha b^\tau_\rho\eta_\tau + b^\rho_\alpha\partial_\rho\eta_3\right), v_3 = \eta_3(x) + w(z)\overline{y}(x), \\ v_3 &= \eta_3(x) + w(z)\overline{y}(x), \\ E^w(u, v) &= \int_S\left(\int_{-h}^{h}\sigma^{ij}(u)\epsilon_{ij}(v)\psi(x, z)\mathrm{d}z\mathrm{d}S\right), \\ L^w(v) &= \int_S\left(\int_{-h}^{h}f^i(x, z, t)v_i\psi(x, z)\mathrm{d}z\right)\mathrm{d}S + \int_\Gamma p^i(x, z, t)v_i\mathrm{d}\Gamma; \\ &= \int_S\left(F^i(x)\eta_i + F^4\overline{y}\right)\mathrm{d}S + \int_{\gamma_1}\left(\mathrm{H}^i(x)\eta_i + \mathrm{H}^4\overline{y}\right)\mathrm{d}\gamma_1 + \int_{\gamma_1}m^\alpha\theta_\alpha d\gamma_1. \end{aligned} \tag{26}$$

Here the stress σ and strain ϵ fields are defined through equations (8)–(13) $(F^i, F^4), (H^i, H^4), m^\alpha, \theta_\alpha$ are,

respectively, resultant surface force, shear force, moment density, and the opposite angle of rotation of a section at the border.

Proof. Resultant forces are also sufficiently smooth and the bilinear form is coercive. Existence and uniqueness of a solution are obtained through the Lax-Milgram lemma.

4. Validation of the Model

In the numerical validation section we will use a finite element that we name "MT6" or "T6-m", which is a modified T6 finite element. Figure 1 below presents the shape of both elements.

Let us consider a shell $\Omega = S \times [-h/2, h/2]$ whose constitutive law is

$$\begin{aligned}\sigma^{ij}(u,q) &= \overline{\lambda}\left(\epsilon_{\alpha}^{\alpha}(u) + \epsilon_{l}^{l}(q)\right)G^{ij} + 2\overline{\mu}\left(\epsilon^{ij}(u) + \epsilon^{ij}(q)\right)\\ &= C^{ijkl}\epsilon_{kl}(u,q).\end{aligned} \tag{27}$$

The variational formulation for a fixed transverse distribution function w,is as follows:

$$\begin{cases}(u(x), \overline{q}(x)) \in U_{\text{ad}},\\ E((u,\overline{q});(v,\overline{y})) = L(v,\overline{y}).\end{cases} \tag{28}$$

For every $(v, \overline{y}), \in U_{\text{ad}}$ with

$$U_{\text{ad}} = \left(H^1_{Y_0}(S)\, xH^1_{Y_0}(S)\, xH^2_{Y_0}(S)\, xH^1_{Y_0}(S)\right). \tag{29}$$

Let $A^{\alpha\beta\delta\tau} = \overline{\lambda}G^{\alpha\beta}G^{\delta\tau} + 2\overline{\mu}G^{\alpha\tau}G^{\tau\beta}$
Then

$$\begin{aligned}E(((u,\overline{q});(v,\overline{y})) &= \int_S\int_{h/2}^{h/2}\sigma^{ij}(u,q)\epsilon_{ij}(v,w\overline{y})\psi \mathrm{d}z\mathrm{d}S\\ &= \int_S\int_{h/2}^{h/2}\left[A^{\alpha\beta\delta\tau}\epsilon_{\delta\tau}(u)\epsilon_{\alpha\beta}(v) + wA^{\alpha\beta\delta\tau}\Upsilon_{\delta\tau}\epsilon_{\alpha\beta}(u)\overline{y} + \overline{\lambda}w'G^{\alpha\beta}\epsilon_{\alpha\beta}(u)\overline{y} + \left(\overline{\lambda}G^{\alpha\beta}w' + wA^{\alpha\beta\delta\tau}\Upsilon_{\delta\tau}\right)\overline{q}\epsilon_{\alpha\beta}(v)\right]\psi \mathrm{d}z\mathrm{d}S\\ &\quad + \int_S\int_{h/2}^{h/2}\left[\left(w^2A^{\alpha\beta\delta\tau}\Upsilon_{\delta\tau}\Upsilon_{\alpha\beta} + \overline{\lambda}ww'^{G^{\alpha\beta}\Upsilon_{\alpha\beta}}\right)\overline{qy} + (\overline{\lambda}+2\overline{\mu})(w')^2\overline{qy} + \overline{\mu}G^{\alpha\beta}w^2\partial_\beta\overline{q}\partial_\alpha\overline{y}\right]\psi \mathrm{d}z\mathrm{d}S.\end{aligned} \tag{30}$$

Let

$$\begin{aligned}D^{\alpha\beta}_{0w} &= \int_{h/2}^{h/2}\left[wA^{\alpha\beta\delta\tau}\Upsilon_{\delta\tau}\right]\psi \mathrm{d}z; D^{\alpha\beta}_{1w},\\ E^{\alpha\beta}_{0w} &= \int_{h/2}^{h/2}\left[\overline{\lambda}\,G^{\alpha\beta}w'\right]\psi \mathrm{d}z; E^{\alpha\beta}_{1w},\\ F^{\alpha\beta}_{0w}(\gamma) &= \int_{h/2}^{h/2}\left[wA^{\alpha\beta\delta\tau}\Upsilon_{\delta\tau} + \overline{\lambda}G^{\alpha\beta}w'\right]\psi \mathrm{d}z; F^{\alpha\beta}_{1w}(\gamma)\\ &\quad \int_{h/2}^{h/2} z\left[wA^{\alpha\beta\delta\tau}\Upsilon_{\delta\tau} + \overline{\lambda}G^{\alpha\beta}w'\right]\psi \mathrm{d}z; F^{\alpha\beta}_{2w}(\gamma),\\ F^{33}_{w0}(\gamma) &= \int_{h/2}^{h/2}\left[w^2A^{\alpha\beta\delta\tau}\Upsilon_{\delta\tau}\Upsilon_{\alpha\beta} + \overline{\lambda}ww'G^{\alpha\beta}\right]\psi \mathrm{d}z; F^{33}_{w1}(\gamma),\\ I^{\alpha\beta}_{ww}(\gamma) &= \int_{h/2}^{h/2}(\overline{\mu})G^{\alpha\beta}(w)^2\psi \mathrm{d}z.\end{aligned} \tag{31}$$

Then an equivalent form of the variational equation is as follows:

$$\begin{aligned}E((u,\overline{q};(v,\overline{y})) &= \int_S\left(N^{\alpha\beta}(u)e_{\alpha\beta}(v) + M^{\alpha\beta}(u)K_{\alpha\beta}(v) + M^{*\alpha\beta}(u)Q_{\alpha\beta}(v)\mathrm{d}S + \int_S\left(D^{\alpha\beta}_{0w}e_{\alpha\beta}(u) - D^{\alpha\beta}_{1w}K_{\alpha\beta}(u) + D^{\alpha\beta}_{2w}Q_{\alpha\beta}(u)\right)\overline{y}\mathrm{d}S\right.\\ &\quad + \int_S\left(E^{\alpha\beta}_{0w}e_{\alpha\beta}(u) - E^{\alpha\beta}_{1w}K_{\alpha\beta}(u) + E^{\alpha\beta}_{2w}Q_{\alpha\beta}(u)\right)\overline{y}\mathrm{d}S + \overline{q}\int_S\left(F^{\alpha\beta}_{0w}(\gamma)e_{\alpha\beta}(v) - F^{\alpha\beta}_{1w}(\gamma)K_{\alpha\beta}(v) + F^{\alpha\beta}_{2w}(\gamma)Q_{\alpha\beta}(v)\right)\mathrm{d}S\\ &\quad + \int_S\overline{q}\,\overline{y}\left(F^{33}_{w0}(\gamma) - F^{33}_{w1}(\gamma) + F^{33}_{w2}(\gamma)\right)dS + \int_S\left(I^{\alpha\beta}_{ww}\partial_\beta\overline{q}\partial_\alpha\overline{y}\right)\mathrm{d}S,\end{aligned} \tag{32}$$

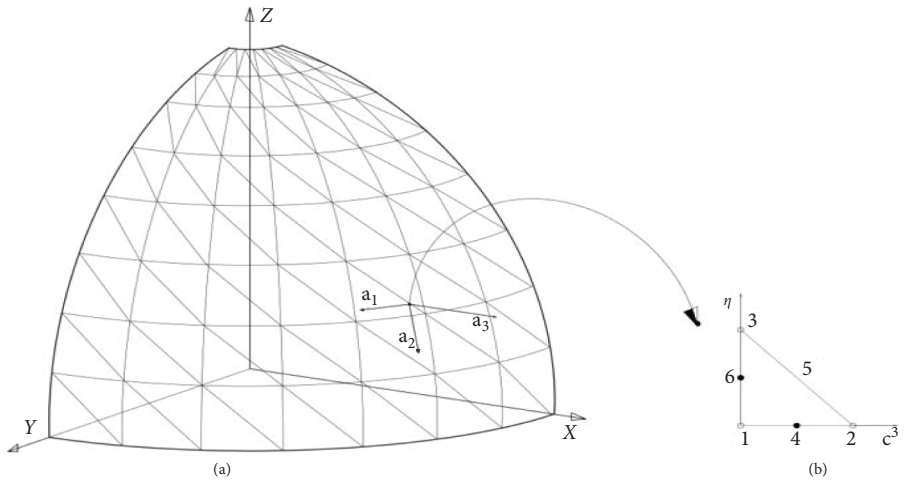

Figure 1: (a) Triangular mesh. (b) MT6 Finite Element.

where by letting $\psi \approx 1, G^{\alpha\beta} \approx a^{\alpha\beta}$ in calculating the efforts, $E, \overline{\nu}$ Young's modulus and Poisson's ratio, respectively,

$$N^{\alpha\beta} = \frac{Eh}{1-\overline{\nu}^2}\left[(1-\overline{\nu})e^{\alpha\beta}(u) + \frac{\overline{\nu}(1-\overline{\nu})}{1-2\overline{\nu}}e^{\rho}_{\rho}(u)a^{\alpha\beta}\right] + \frac{Eh^3}{12\left(1-\overline{\nu}^2\right)}\left[(1-\overline{\nu})Q^{\alpha\beta}(u) + \frac{\overline{\nu}(1-\overline{\nu})}{1-2\overline{\nu}}Q^{\rho}_{\rho}(u)a^{\alpha\beta}\right],$$

$$M^{\alpha\beta} = \frac{Eh^3}{12\left(1-\overline{\nu}^2\right)}\left[(1-\overline{\nu})K^{\alpha\beta}(u) + \frac{\overline{\nu}(1-\overline{\nu})}{1-2\overline{\nu}}K^{\rho}_{\rho}(u)a^{\alpha\beta}\right],$$

$$M^{*\alpha\beta} = \frac{Eh^5}{80\left(1-\overline{\nu}^2\right)}\left[(1-\overline{\nu})Q^{\alpha\beta}(u) + \frac{\overline{\nu}(1-\overline{\nu})}{1-2\overline{\nu}}Q^{\rho}_{\rho}(u)a^{\alpha\beta}\right] + \frac{Eh^3}{12\left(1-\overline{\nu}^2\right)}\left[(1-\overline{\nu})e^{\alpha\beta}(u) + \frac{\overline{\nu}(1-\overline{\nu})}{1-2\overline{\nu}}e^{\rho}_{\rho}(u)a^{\alpha\beta}\right], \tag{33}$$

$$\overline{\lambda} = \frac{E\overline{\nu}}{(1-2\overline{\nu})(1+\overline{\nu})}; \overline{\mu} = \frac{E}{2(1+\overline{\nu})},$$

$$L(v, \overline{y}) = \int_S \left(\overline{P}^i v_i + \overline{P}^4 \overline{y}\right)\mathrm{d}S + \int_{\gamma_1}\left(q^i v_i + q^4 \overline{y}\right)\mathrm{d}\gamma + \int_{\gamma_1}\left(m^{\alpha}\theta_{\alpha}(v)\right)\mathrm{d}\gamma,$$

where

$$\overline{P}^4 = \int_{h/2}^{h/2} f^3 w\,\mathrm{d}z + w\left(\frac{h}{2}\right)\overline{p}^3_{+} - w\left(-\frac{h}{2}\right)\overline{p}^3_{-}. \tag{34}$$

We use iso-parametric Lagrangian symplectic type triangle finite elements which are based on complete polynomial bases [23]. The finite element used has 4 (four) degrees of freedom at the vertex nodes (3 displacements and 1 stretching) and 1 (one) additional degree of freedom at mid-points of edges (1 for transverse displacement). By laying the matrix of shape functions we get

$$N = \begin{bmatrix} 1-\xi-\eta & \xi & \eta & 0 & 0 & 0 & 0 & 0 & 0 & 0 & 0 & 0 & 0 & 0 \\ 0 & 0 & 0 & 1-\xi-\eta & \xi & \eta & 0 & 0 & 0 & 0 & 0 & 0 & 0 & 0 \\ 0 & 0 & 0 & 0 & 0 & 0 & -(1-\xi-\eta)(1-2(1-\xi-\eta)) & -\xi(1-2\xi) & -\eta(1-2\eta) & 4(1-\xi-\eta)\xi & 4\xi\eta & 4(1-\xi-\eta)\eta & 0 & 0 \\ 0 & 0 & 0 & 0 & 0 & 0 & 0 & 0 & 0 & 0 & 0 & 0 & (1-\xi-\eta) & \xi \quad \eta \end{bmatrix}, \tag{35}$$

$${}^{t}\widehat{U}_e = [\widehat{u}_1\ \widehat{u}_2\ \widehat{u}_3\ \widehat{v}_1\ \widehat{v}_2\ \widehat{v}_3\ \widehat{w}_1\ \widehat{w}_2\ \widehat{w}_3\ \widehat{w}_4\ \widehat{w}_5\ \widehat{w}_6\ \ \widehat{q}_1\ \widehat{q}_2\ \widehat{q}_3].$$

4.1. Hemisphere under Diametrically Opposed Loads. This test case makes it possible to verify the behavior of the element in bending and shear [26]. The test of a thin hemisphere ($R/h = 250$) subjected to a free base with four concentrated charges (see Figure 2) is used to verify the absence of membrane locking [21]. The reference solution presented by [27] gives displacements according to the direction of the load: $U_A = V_B = 0.094$ mm. Due to symmetry considerations, only a quarter of the hemisphere is meshed. The mesh is regular and the number of elements varies from

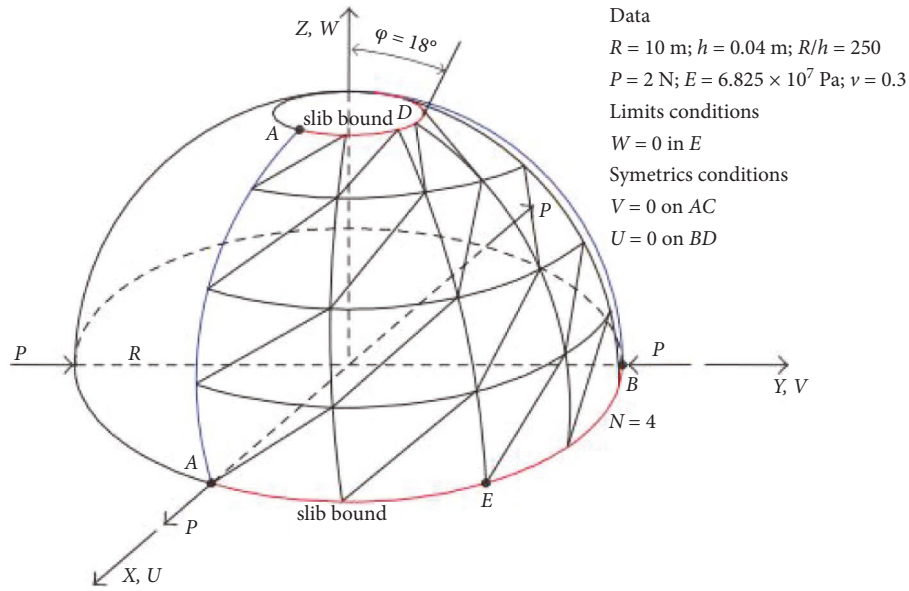

Figure 2: Hemispheric shell benchmark.

2 to 15. We compare our results obtained with the MT6 or T6-m to several families of finite elements of shells. In Figure 3, the displacement convergence at U_A according to the number of elements is represented in Table 1. This new model of thick shell does not have a locking problem. In addition, it is memory less greedy and fast converging with very few elements, as shown in Figure 3 for a thin shell.

4.2. Pinched Cylinder. The aim of this test is to check the behavior of the element (cylindrical shell) in bending and shearing. It has been studied by several authors ([21, 27–30]). The two ends of the shell are closed by an infinitely rigid diaphragm. An eighth of the cylinder is meshed thanks to the symmetries of the problem. The shell is subjected to a concentrated load at point A, $\|\overrightarrow{P}\| = 1$ (Figure 4). Geometry, loading, and material data for this test case are listed in Table 2. And comparison is provided in Table 3.

$$\overline{W}_C = -\frac{W_C.E.h}{P} = 164.24. \tag{36}$$

4.3. Sphere under Uniform Pressure. The geometric and mechanical parameters of the hollow sphere under consideration are defined in Table 4.

The solution is obtained by solving the equilibrium equation in the absence of volume force:

$$\frac{\partial \sigma_{rr}}{\partial r} - \frac{2}{r}\left(\sigma_{rr} - \sigma_{\theta\theta}\right) = 0, \tag{37}$$

where σ_{rr}, $\sigma_{\theta\theta}$ are the radial and circumferential components of the stress tensor.

It is shown that the solution is in the form $u_r = Ar^{\lambda_1} + Br^{\lambda_2}$ [31].

With:

$$\begin{aligned}
\lambda_1 &= -\frac{1}{2}\left(-1 + \frac{\overline{\lambda}}{(2\overline{\mu}+\overline{\lambda})}\right) + \frac{1}{2}\sqrt{\left(-1 + \frac{\overline{\lambda}}{(2\overline{\mu}+\overline{\lambda})}\right)^2 - 4\left(-\left(2 - \frac{\overline{\lambda}}{(2\overline{\mu}+\overline{\lambda})}\right)\right)},\\
\lambda_2 &= -\frac{1}{2}\left(-1 + \frac{\overline{\lambda}}{(2\overline{\mu}+\overline{\lambda})}\right) - \frac{1}{2}\sqrt{\left(-1 + \frac{\overline{\lambda}}{(2\overline{\mu}+\overline{\lambda})}\right)^2 - 4\left(-\left(2 - \frac{\overline{\lambda}}{(2\overline{\mu}+\overline{\lambda})}\right)\right)},\\
B &= -\frac{(2\overline{\mu}+\overline{\lambda})\lambda_1 R_i^{\lambda_1-1} + \overline{\lambda}R_i^{\lambda_1-1}}{(2\overline{\mu}+\overline{\lambda})\lambda_2 R_e^{\lambda_2-1} + \overline{\lambda}R_e^{\lambda_2-1}}A,\\
A &= -\frac{P_i}{(2\overline{\mu}+\overline{\lambda})\lambda_1 R_i^{\lambda_1-1} + \overline{\lambda}R_i^{\lambda_1-1}} - \frac{(2\overline{\mu}+\overline{\lambda})\lambda_2 R_i^{\lambda_2-1} + \overline{\lambda}R_i^{\lambda_2-1}}{(2\overline{\mu}+\overline{\lambda})\lambda_1 R_i^{\lambda_1-1} + \overline{\lambda}R_i^{\lambda_1-1}}B.
\end{aligned} \tag{38}$$

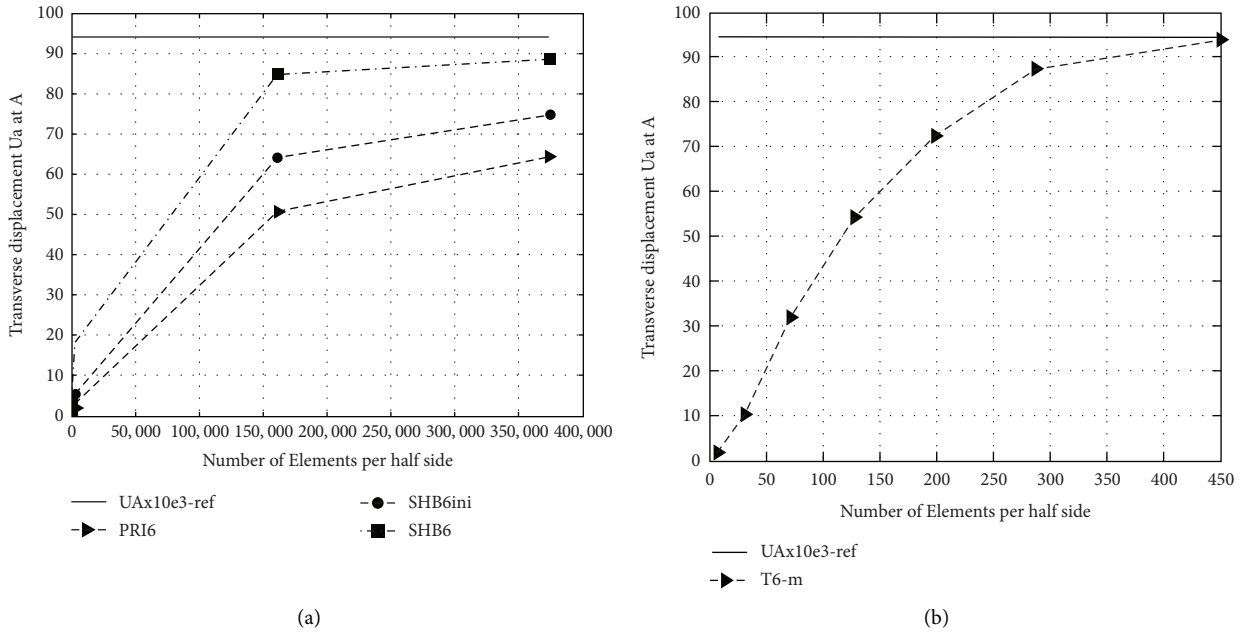

Figure 3: (a) Convergence of displacements at point A(3D Model), (b) convergence of displacements at point A (2D Model).

Table 1: Hemisphere under diametrically opposite loads, displacement $U_A \times 10^3$.

Reference: $U_A \times 10^3 = 94$ mm					
	Family of 3D elements			Family of 2D elements	
Mesh step 3D model	PRI6	SHB6 initial	SHB6	Mesh step 2D model	T6_M
3×(5×5×1)×2	0,104	0,589	1,60	2×2×2	1, 8
3×(11×11×1)×2	0,457	1,209	4,27	4×4×2	10, 27
3×(22×22×1)×2	2,015	5,424	18,05	6×6×2	31, 92
3×(180×180×1)×2	50,72	64,18	84,70	8×8×2	54, 35
3×(250×250×1)×2	64,35	74,82	88,40	10×10×2	72, 33
				12×12×2	87, 26
				15×15×2	93, 6
				16×16×2	94. 8

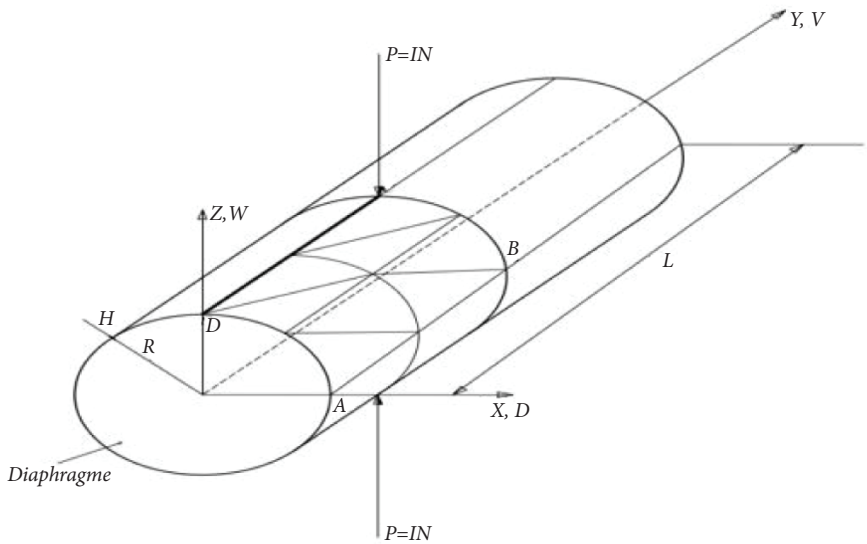

Figure 4: Geometry and loading of the clamped cylindrical shell with diaphragm.

Table 2: Geometry and mechanical data of the pinched cylinder.

Length	$L = 6\,\text{m}$
Radius	$R = 3\,\text{m}$
Thickness	$h = 0.03\,\text{m}$
Young's modulus	$E = 3 \times 10^{10}\,\text{Pa}$
Poisson's coefficient	$\nu = 0.3$
Limit conditions	$U = W = 0$ on AD
Conditions of symetry	$W = 0$ on AB; $V = 0$ on BC; $U = 0$ on CD
Sollictation at C	$f = -0.25\,\text{N}$

Table 3: Transverse displacements results W_C at point C.

Reference: $\overline{W}_C = -W_C.E.h/P = 164.24$					
Mesh step 3D model	PRI6	SHB6 initial	SHB6	Mesh step 2D model	T6_M
$(10 \times 10 \times 1) \times 2$	10,134	16,335	39,411	$2 \times 2 \times 2$	9,79
$(30 \times 30 \times 1) \times 2$	35,919	57,33	107,82	$4 \times 4 \times 2$	43,32
$(50 \times 50 \times 1) \times 2$	60,696	89,973	137,79	$6 \times 6 \times 2$	74,08
$(70 \times 70 \times 1) \times 2$	80,406	112,95	151,83	$8 \times 8 \times 2$	96,09
$(90 \times 90 \times 1) \times 2$	95,31	129,06	159,3	$10 \times 10 \times 2$	116,47
				$12 \times 12 \times 2$	135,23
				$15 \times 15 \times 2$	155,01
				$16 \times 16 \times 2$	158,75
				$18 \times 18 \times 2$	163,38

Table 4: Geometry and mechanical data of the sphere under uniform pressure.

Inner radius	$R_i = 10\,\text{cm}$
Outer radius	$R_e = 20\,\text{cm}$
Thickness	$h = R_e - R_i$
Young's modulus	$E = 21\,\text{MPa}$
Poisson's coefficient	$\nu = 0.3$
Inner pressure	$P_i = 0.1\,\text{MPa}$
Outer pressure	$P_e = 0\,\text{MPa}$

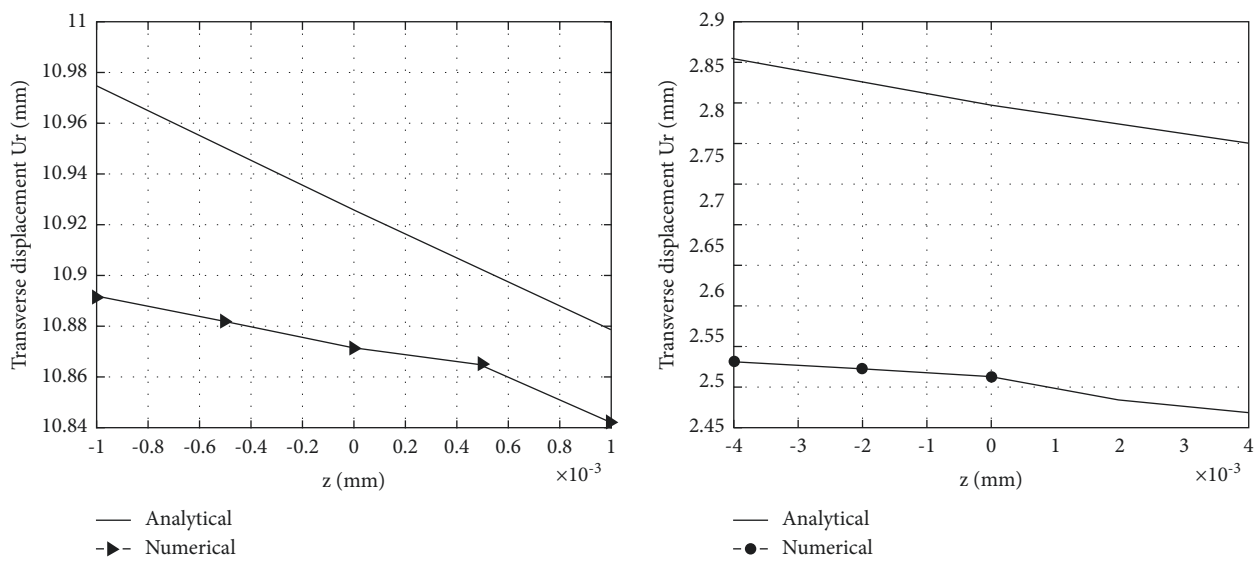

Figure 5: Continued.

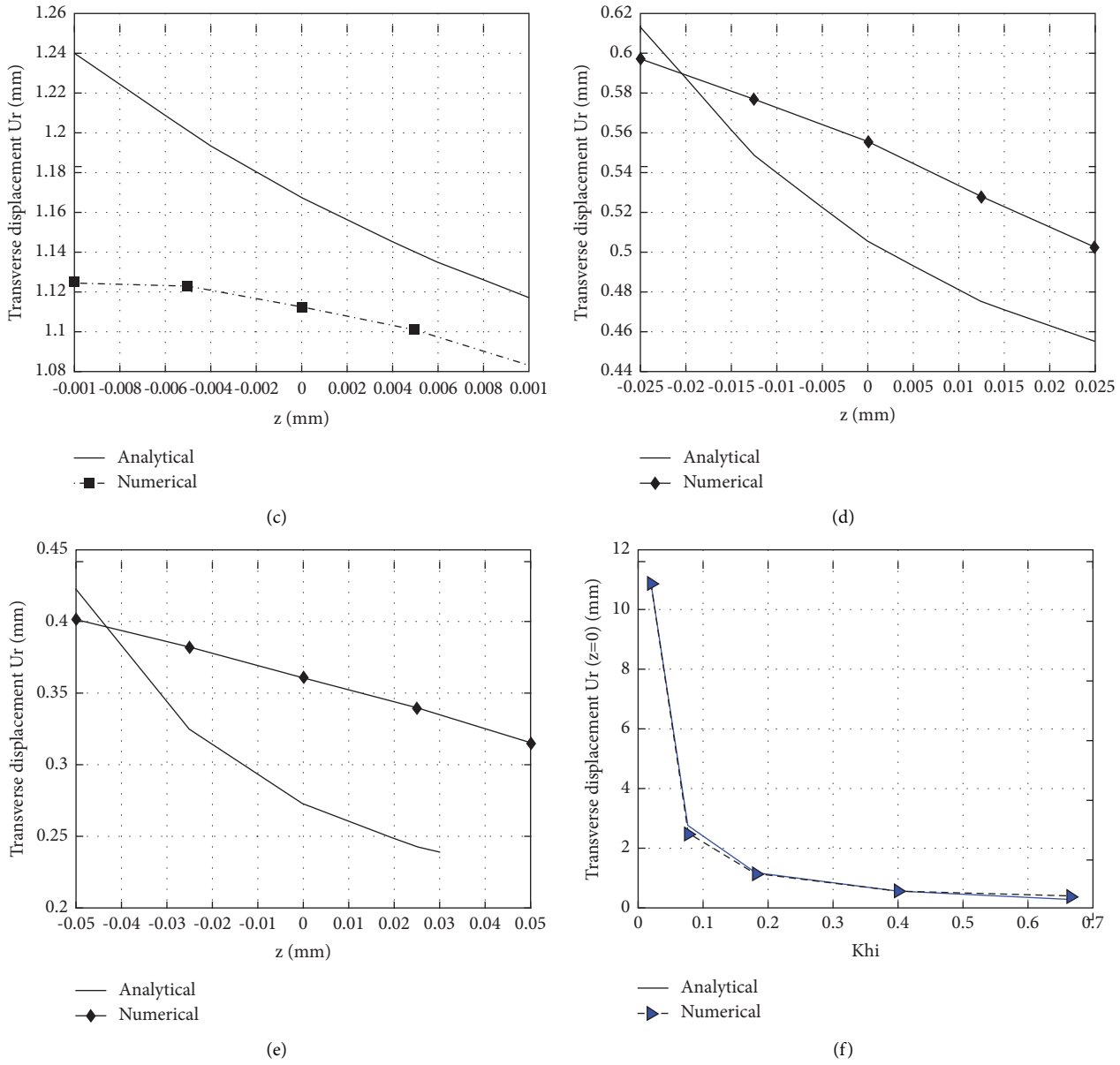

Figure 5: (a) Evolution of radial deviation as a function of thickness ratio (khi = 0.0198). (b) Evolution of radial deviation as a function of thickness ratio (khi = 0.0769), (c) evolution of radial deviation as a function of thickness ratio (khi = 0.1818). (d) Evolution of radial deviation as a function of thickness ratio (khi = 0.4), (e) evolution of radial deviation as a function of thickness ratio (khi = 0.667). (f) Evolution of the radial deviation of the mid-surface as a function of the thickness ratio khi.

The superposition curves shown in Figures 5(a)–5(f) and Table 5 show the deviations.

5. Discussions

The shell model, the "N" model [18], is used for the calculation of the hemisphere (Figure 2 and (Table 1), the pinched cylinder (Figure 4 and Table 2) and the sphere under uniform pressure (Table 4). The finite element of the triangular type uses stretching as a degree of freedom to follow the displacement in the thickness. Several authors have worked on the hemisphere case using triangular, rectangular, and even volume finite elements, where all displacement components are represented by polynomials of order 2 and 3. In [26], it is indicated that the results obtained with the new SHR6 element converge faster than the initial PRI6 and SHR6 does not lock for the same number of elements. However, this 3D element has an excessively high number of degrees of freedom as the thickness of the shell increases. It would therefore require a significant computational effort to perform the analysis using this element. In comparison, the present element uses only four degrees of freedom per vertex node and one for middle nodes. The hemispherical shell described above is analyzed here using

Table 5: Radial deviation of the shell (analytical and numerical model) according to the ratio h/R, h is the thickness.

Ratio h/R	0.0198			0.0769			0.1818			0.4			0.667		
z	Analytical (mm)	Numerical (mm)	Error (%) (A-N)/A	Analytical (mm)	Numerical (mm)	Error (%) (A-N)/A	Analytical (mm)	Numerical (mm)	Error (%) (A-N)/A	Analytical (mm)	Numerical (mm)	Error (%) (A-N)/A	Analytical (mm)	Numerical (mm)	Error (%) (A-N)/A
$-h/2$	10,9746	10,891	0.76	2,8554	2,481	13.11	1,241	1,1252	9.33	0,6129	0,5969	2.60	0,4222	0,4012	4.97
$-h/4$	10,9497	10,882	0.62	2,8252	2,473	12.47	1,200	1,1227	6.50	0,5489	0,5768	5.09	0,3247	0,3815	17.49
0	10,9253	10,871	0.50	2,7976	2,462	12.00	1,167	1,1125	4.70	0,5052	0,5554	9.94	0,2719	0,3602	32.47
$h/4$	10,9016	10,865	0.34	2,7725	2,435	12.17	1,140	1,1014	3.39	0,4752	0,5274	10.98	0,2421	0,3395	40.23
$h/2$	10,8784	10,842	0.33	2,7496	2,419	12.02	1,117	1,0841	3.01	0,455	0,5024	10.42	0,2254	0,3154	39.92

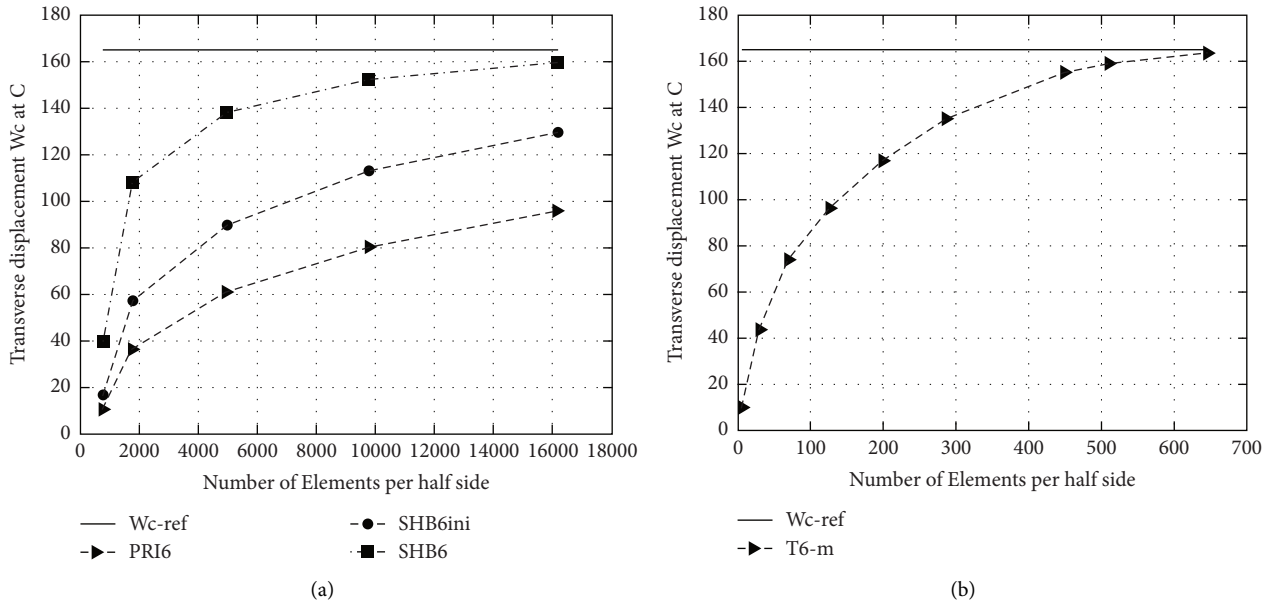

Figure 6: (a) Convergence of displacements at point C (3D model) (b) convergence of displacements at point C (2D model).

the triangular element presented above. The results from the analyses are compared with those obtained from the solution given in [27]. Convergence tests were carried out for the normal deviation at point A (Figure 3) of the shell. Table 1 shows that MT6 with the model "N" indicates a deviation of 0.42% for a mesh of $15 \times 15 \times 2$, which is reached by CSFE3-sh with a mesh of $12 \times 12 \times 2$ to converge to the reference solution. The DKT12 and DKT18 give 2% and 1.06% with a mesh of $12 \times 12 \times 2$ for the reference solution [20]. As for the SHR6 developed in [26] the difference obtained is 4.49% for a mesh of $3 \times (250 \times 250 \times 1) \times 2$ or 375 000 elements. We realize that compared to the "N" model, this volumetric model [26], which also takes into account the variation of thickness, is very memory greedy and calculating time is excessive. Figure 3 shows an excellent agreement between the results obtained with the element MT6 and those found in the literature for the variation of the normal deviation at point A.

The pinched cylinder is a reference example for testing a finite element model, especially for thin shells. The loading case here is not symmetrical (due to the concentrated point load) and the solution cannot be managed by the 3D elasticity theory [20]. The "N" model although being a thick shell model, shows good convergence towards the reference solution. The error is 0.523% for a mesh of $18 \times 18 \times 2$, while the SHR6 of [26] indicates an error of 3% for a mesh of $(90 \times 90 \times 1) \times 2$ or 16200 elements. The convergence curves are illustrated in (Figures 6(a) and 6(b)). It is a difficult problem to solve numerically when the thickness is small because the locking and hourglass problems are recurrent. The finite element of [26] does not lock, but it needs a very fine mesh and fairly important calculating time.

The sphere case under uniform pressure is a resolvable case by the 3D elasticity theory. The reference solution, which is a function of the radius, is obtained analytically. The model "N" (by Nzengwa [18]) has the ability to also calculate the radial displacement as a function of the radius. In Table 5, we plotted the following values of the characteristic parameter: $h/R = 0.0198$, 0.0769, 0.1818, 0.4, and 0.667. A gap of less than 5.55% was observed between the inner and outer radii for the radial deviation for thin shells (example $h/R = 0.0198$). In general, the average gap is around 10%, as shown in (Figures 5(a)–5(e)). The numerical displacements are smaller than the analytical ones, which highlights the contribution of the flectional energy of the double curvature shell. Table 5 shows that the model is closer to the reference solutions according to the ratio khi for a uniform loading. For nonuniform loads, the 3D elasticity theory can no longer be able to provide analytical solutions, while the model "N" still remains efficient for solving common problems in complex shell structures, either thin or thick.

6. Conclusion

The 2D model "N" which is a 4-parameter model has proven its efficiency in handling different loadings in thin or thick shells with the calculation of transverse stresses, strains, and also thickness variation. Increasing the degree of the polynomial of the transverse stretch distribution function $w(z)$ does not increase the number of parameters. The transverse distribution function $w(z)$ is not limited to polynomials only. The model includes terms found in the classical theory of thin or thick shells and seems to be suitable for stiffened shells that are actually locally thin or thick shell structures. The distribution function $w(z)$ in this paper is z, so the quality of the results can be improved by choosing another expression, which makes the model flexible.

Data Availability

No data were used to support this study.

Conflicts of Interest

The authors declare that they have no conflicts of interest.

References

[1] P. Naghdi, "The theory of shells and plates," *Hanbuch der Physik*, vol. 2, pp. 425–640, 1970.

[2] T. Vuong Dieu and F. C. A. Abel-Meraim, "A New Assumed Strain Solid–Shell Formulation," *Journal of mechanical science and technology*, vol. 25, 2011.

[3] V. V. Novozhilov, "The Theory of Thin Elastic Shells," *Noordhoff. Moscow*, vol. 164, 2021.

[4] A. E. H. Love, "The small free vibrations and deformation of a thin elastic shells," *Philosophical Transactions of the Royal Society of London*, vol. 179, pp. 491–546, 1888.

[5] G. Kirchhoff, "Uber das gleichgewicht und die bewegung einer elastischen scheibe," *Journal für die Reine und Angewandte Mathematik*, vol. 40, pp. 51–88, 1850.

[6] A. W. Leissa, *Vibration of Shells*, NASA, Washington D.C, 1973.

[7] M. Malikan, M. Krasheninnikov, and V. A. Eremeyev, "Torsional stability capacity of a nano-composite shell based on a nonlocal strain gradient shell model under a three-dimensional magnetic field," *International Journal of Engineering Science*, vol. 148, Article ID 103210, 2020.

[8] R. D. Mindlin, "Influence of rotatory inertia and shear on flexural motions of isotropic, elastic plates," *Journal of Applied Mechanics*, vol. 18, no. 1, pp. 31–38, 1951.

[9] E. Reissner, "The effect of transverse shear deformation on the bending of elastic plates," *Journal of Applied Mechanics*, vol. 12, no. 2, pp. 69–77, 1945.

[10] E. Reisnner, "Small Bending and Stretching of sandwich-type Shells," *Massachusetts Institure of Technology*, vol. 23, 1949.

[11] F. Mehralian, Y. Tadi Beni, and M. Karimi Zeverdejani, "Nonlocal strain gradient theory calibration using molecular dynamics simulation based on small scale vibration of nanotubes," *Physica B: Condensed Matter*, vol. 514, pp. 61–69, 2017.

[12] A. Ghorbanpour Arani, M. Abdollahian, R. Kolahchi, and A. H. Rahmati, "«Electro-thermo-torsional buckling of an embedded armchair DWBNNT using nonlocal shear deformable shell model," *Composites Part B: Engineering*, vol. 51, pp. 291–299, 2013.

[13] M. H. Shojaeefard, M. Mahinzare, H. Safarpour, H. Saeidi Googarchin, and M. Ghadiri, "Free vibration of an ultra-fast-rotating-induced cylindrical nano-shell resting on a Winkler foundation under thermo-electro-magneto-elastic condition," *Applied Mathematical Modelling*, vol. 61, pp. 255–279, 2018.

[14] A. Ibrahimbegović, "Nonlinear shell theory with finite rotations and finite strains: recent achievements," in *Proceedings of the. Shell Structures Theory and Application 8th International Conference*, Gdansk, July 2005.

[15] H. Murakami, "Laminated composite plate theory with improved in-plane responses," *Journal of Applied Mechanics*, vol. 53, no. 3, pp. 661–666, 1986.

[16] E. Carrera, S. Valvano, and M. Filippi, "Classical, Higher-Order, Zig-Zag and Variable Kinematic Shell Elements for the Analysis of Composite Multilayered Structures," *European Journal of Mechanics*, vol. 12, 2018.

[17] R. Nzengwa and B. Simo, "A two dimensional model for linear elastic thick shells," *International Journal of Solids and Structures*, vol. 36, no. 34, pp. 5141–5176, 1999.

[18] R. Nzengwa, "Asymptotic 2D-modelling for dynamics of linear elastic thick shell," in *Proceedings of the Shell Structures Theory and Application 8th International Conference*, pp. 157–161, Gdansk, Poland, September 2005.

[19] J. N. Anyi, R. Nzengwa, J. C. Amba, and C. V. Ngayihi Abbe, "Approximation of Linear Elastic Shells by Curved Triangular Finite Elements Based on Elastic Thick Shells Theory," *Mathematical problem engineering*, vol. 2016, pp. 1–12, Article ID 8936075, 2016.

[20] J. N. Anyi, J. C. Amba, D. Essola, N. A. Claude Valery, M. B. Momha, and R. Nzengwa, "«Generalised assumed strain curved shell finite elements (CSFE-sh) with shifted-Lagrange and application on N-T's shells theory," *DE GRUYTER,Curved and Layered Structures*, vol. 7, pp. 125–138, 2020.

[21] J. N. Anyi, A. T. Pouakam, J. C. Amba et al., "Investigation of the macroscopic behaviour of laminates shells (MBLS) under varying loads using low order CSFE-sh FEM and the N-T's 2D shell equations," *Jounal Plos one*, vol. 17, no. 5, Article ID e0267480, 2022.

[22] B. M. Merlin, D. K. Landry, A. J. Chills, N. A. Joseph, Z. Ambassa, and N. Robert, "Investigation of differential shrinkage stresses in a revolution shell structure due to the evolving parameters of concrete," *DE GRUYTER, Curved and Layered structures*, vol. 23, 20168.

[23] D. K. Landry, B. momha Merlin, A. J. Chills et al., "«Experimental measurement and numerical predictions of thickness variation and transverse stresses in a concrete ring," *DE GRUYTER, Curved and Layered structures*, vol. 365, 2020.

[24] A. Blouza and H. Le Dret, "Existence and uniqueness for the linear Koiter model for shells with little regularity," *Comptes Rendus de l'Académie des Sciences (CRAS) Paris, Séries I*, vol. 317, pp. 327–329, 1995.

[25] M. Bernadou and P. G. Ciarlet, "Sur l'ellipticité du modèle linéaire des coques de W.T. Koiter Computing Methods in Sciences and Engineering," *Lecture notes in Economics and systems*, vol. 34, pp. 89–136, 1976.

[26] V.-D. Trinh, *Formulation, développement et validation d'éléments finis de type coques volumiques sous-intégrés stabilisés utilisables pour des problemes a cinématique et comportement non linéaires*, China, 2009.

[27] R. H. Macneal and R. L. Harder, "A proposed standard set of problems to test finite element accuracy," *Finite Elements in Analysis and Design*, vol. 1, no. 1, pp. 3–20, 1985.

[28] R. J. Alves de Sousa, R. P. R. Cardoso, R. A. Fontes Valente, J. W. Yoon, J. J. Gracio, and R. M. Natal Jorge, "A new one-point quadrature enhanced assumed strain (EAS) solid–shell element with multiple integration points along thickness: Part I – geometrically linear applications," *International Journal for Numerical Methods in Engineering*, vol. 62, no. 7, pp. 952–977, 2005.

[29] K. D. Kim, G. Z. Liu, and S. C. Han, "A resultant 8-node solid–shell element for geometrically nonlinear analysis," *Computational Mechanics*, vol. 35, no. 5, pp. 315–331, 2005.

[30] H. Stolarski, T. Belytschko, N. Carpenter, and J. Kennedy, "A simple triangular curved shell element," *Engineering Computations*, vol. 1, no. 3, pp. 210–218, 1984.

[31] M. Methia, A. Benslimane, S. Bouzidi et al., "Analyse des contraintes et des déplacements dans une sphère FGM sous pressions," in *Proceedings of the International Conference on Advanced Mechanics and Renewable Energies*, Boumerdes-Algeria, June 2018.